Supporting information

Electrostatic-Driven Activity, Loading, Dynamics and Stability of a Redox Enzyme on Functionalized-Gold Electrodes for Bioelectrocatalysis

Vivek Pratap Hitaishi,[a] Ievgen Mazurenko,[b] Malek Harb,[a] Romain Clément,[a] Marion Taris,[c] Sabine Castano,[c] David Duché,[d] Sophie Lecomte,[c] Marianne Ilbert,[a] Anne de Poulpiquet,[a] Elisabeth Lojou*[a]

[a] *Aix-Marseille Univ, CNRS, BIP, UMR 7281, 31 Chemin Aiguier, 13009 Marseille, France*

[b] *School of Biomedical Sciences, University of Leeds, LS2 9JT Leeds, UK*

[c] *Institute for Chemistry and Biology of Membrane and Nano-objects, Allée Geoffroy St Hilaire, 33600 Pessac, France*

[d] *Aix Marseille Univ, CNRS, University of Toulon, IM2NP UMR 7334, 13397 Marseille, France*

**Corresponding author: lojou@imm.cnrs.fr*

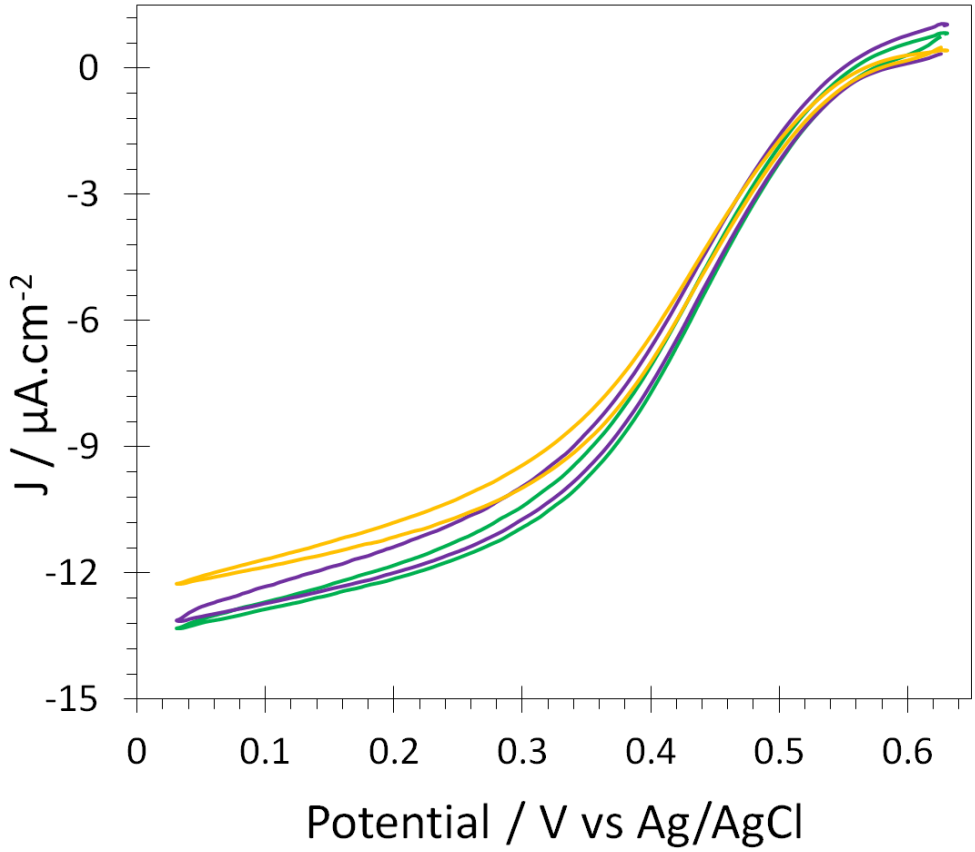

Figure S1 : CVs showing catalytic responses at pH 6 at different scan rates: 5 $mV.s^{-1}$ (green), 10 $mV.s^{-1}$ (purple), 2 $mV.s^{-1}$ (yellow) with *Mv* BOD adsorbed at pH 6 on 6-MHA-SAM.

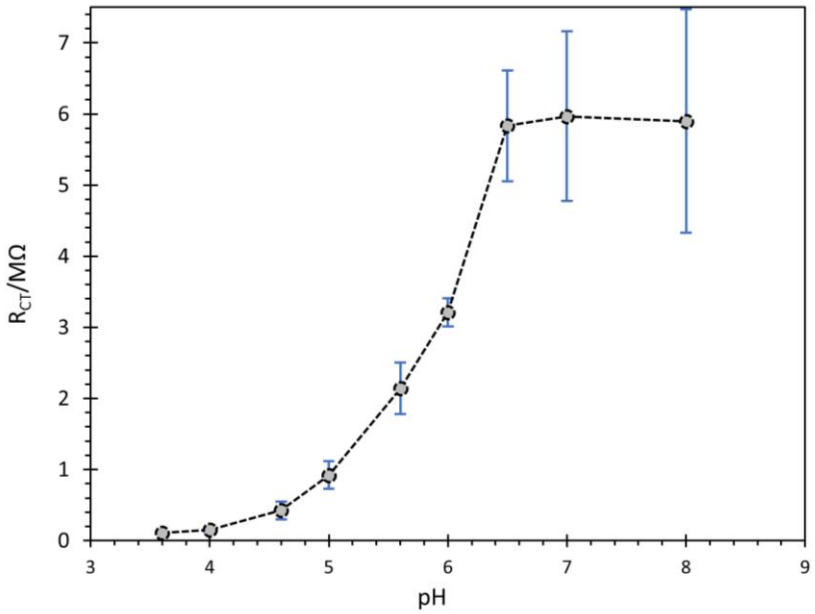

Figure S2: **Determination of the pKa of 6-MHA-SAM.** Determination of the pKa of 6-MHA-SAM by impedance spectroscopy: charge transfer resistance (R_{CT}) was measured in the presence of 1 mM $Fe(CN)_6^{3-/4-}$ in various pH solutions.

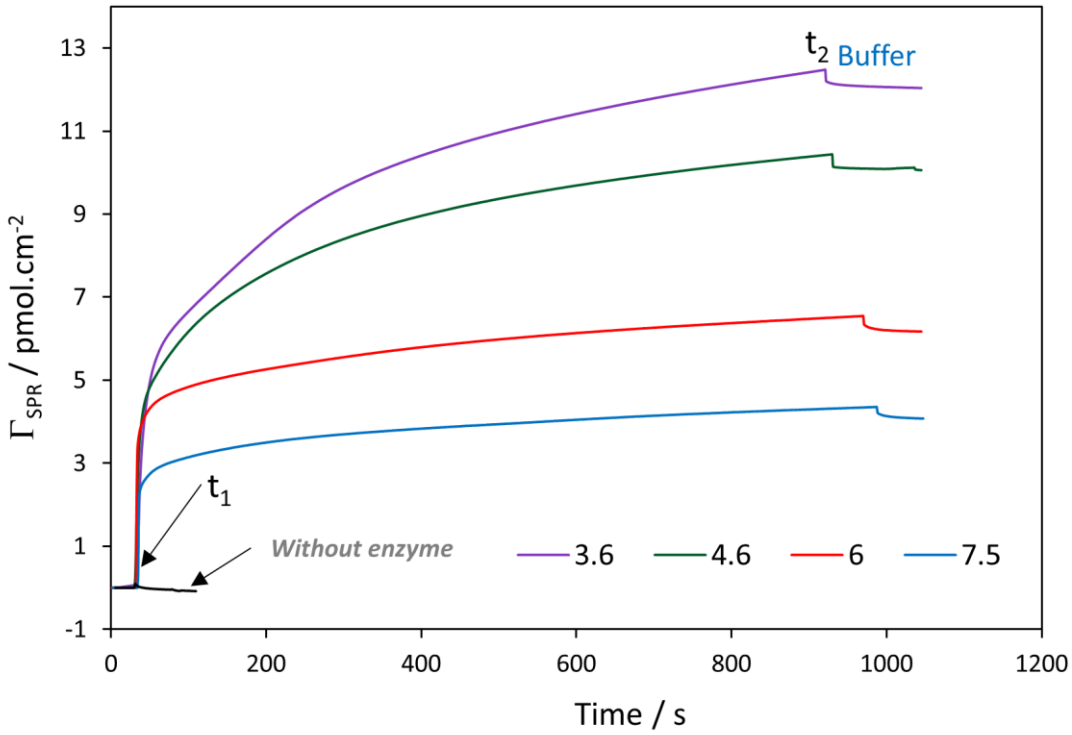

Figure S3. SPR determination of enzyme coverage as a function of pH. SPR measurement of *Mv* BOD adsorption on SPR chip modified by MHA-SAM in 100 mM air-saturated phosphate/phosphate-citrate buffer at desired pHs for 15 min at RT. 20 µM *Mv* BOD was injected at t_1, and the chip was rinsed with buffer at t_2.

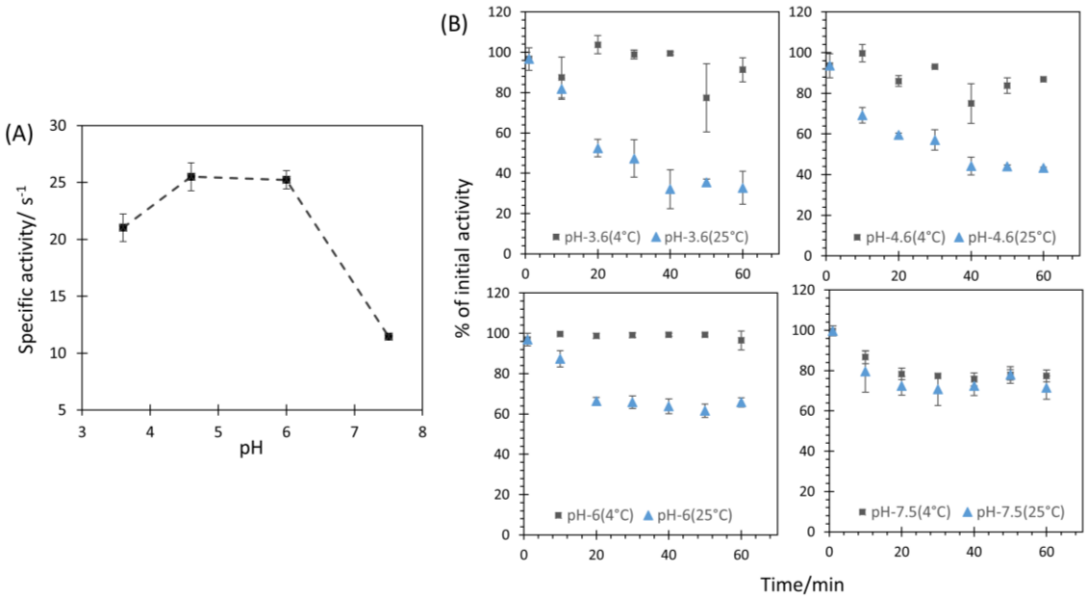

Figure S4. **Comparative stability of the homogeneous activity at RT or 4°C as a function of pH.** (A) Homogeneous activity of freshly prepared *Mv* BOD solution as a function of pH; (B) Remaining homogeneous activity as a function of pH, T° and time (in % of the initial activity).

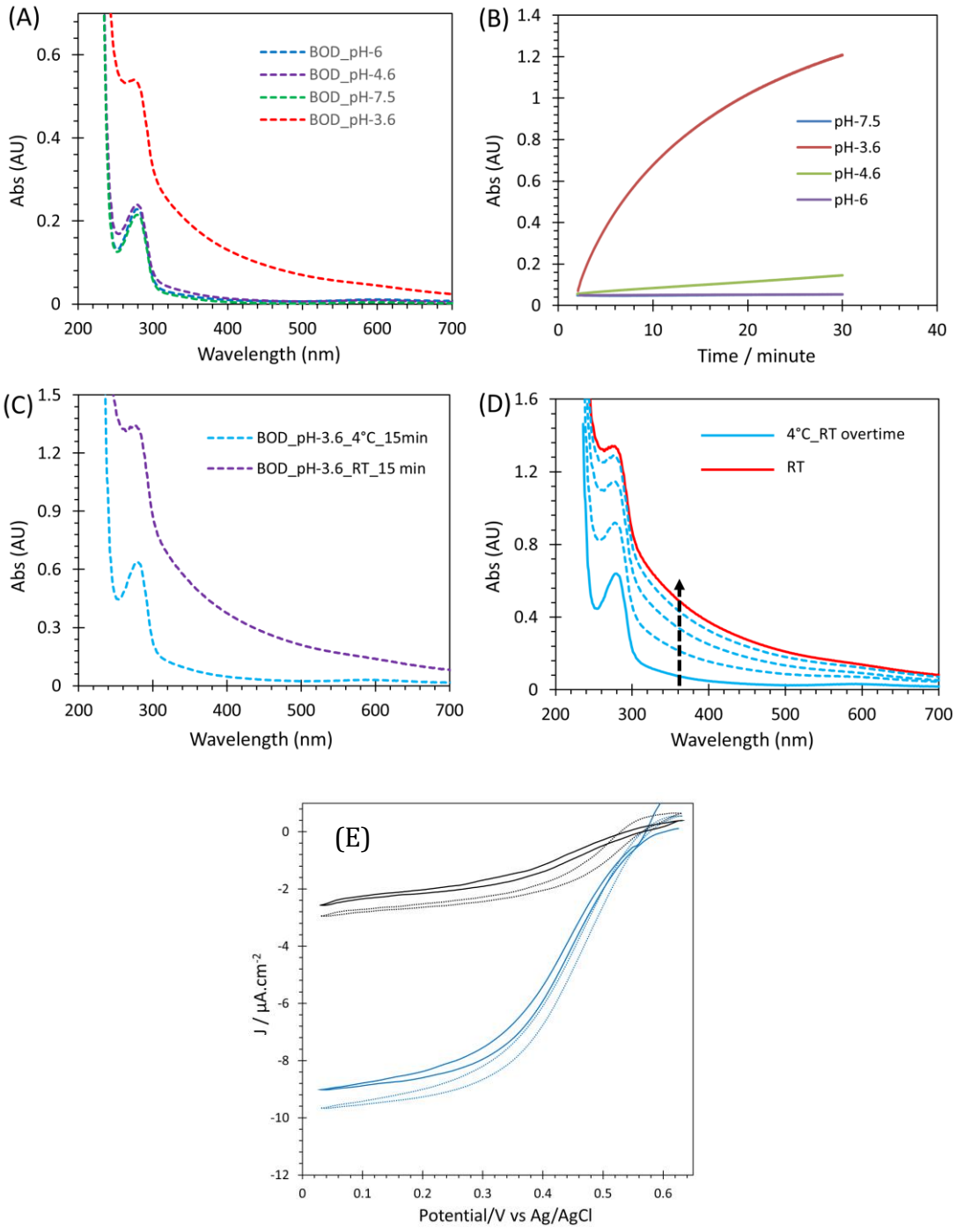

Figure S5. **Temperature and pH dependency of *Mv* BOD aggregation.** (A) UV-Vis spectra of 20 µM *Mv* BOD incubated 15 min in different pH buffers at RT; (B) Kinetics of aggregation of 20 µM *Mv* BOD at RT measured by UV-absorption at 360 nm in different buffer; (C) UV-Vis spectra of 20 µM *Mv* BOD incubated 15 min at

pH 3.6 either at room temperature (RT) or at 4°C; (D) After more than 5 hours of incubation of 20 µM *Mv* BOD at 4°C and pH 3.6, aggregation of BOD can be followed overtime as soon as proteins are incubated at RT. Each blue dotted curve represents a spectrum measured for increasing times (5, 10, 15 min); (E) CVs of O_2 reduction at pH 6 by 20 µM *Mv* BOD adsorbed for 15 min on 6-MHA-SAM at pH 3.6 either at 4°C (black curves) or at RT (blue curves). Dotted lines are obtained after 50 µM ABTS addition in solution.

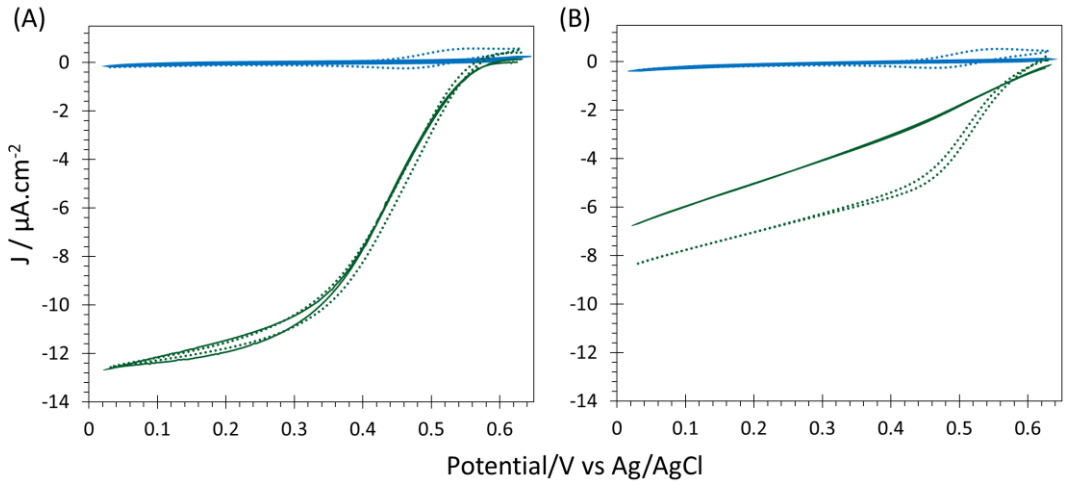

Figure S6. Control experiments on 6-MHA-SAMs using unfolded *Mv* BOD. Catalytic responses at (A) pH 6 or (B) pH 3.6 while *Mv* BOD was heated at 100°C during 15 min in the presence (blue solid) or absence (green solid) of 8 M urea and adsorbed at pH 6 on 6-MHA SAM. Dotted curves represent the corresponding MET signal after the addition of 50 µM ABTS in the electrolyte. Scan rate v = 5 $mV.s^{-1}$.

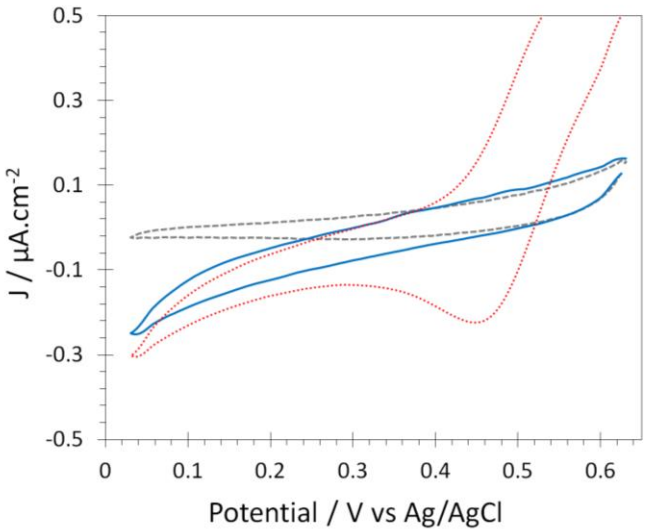

Figure S7. Control experiments on 6-MHA-SAMs using denaturated *Mv* BOD. Catalytic responses at pH 6 with *Mv* BOD adsorbed at pH 6 on 6-MHA SAM after heating the enzyme sample at 100°C for 20 minutes (blue solid). Dotted red curve represents the corresponding MET signal after the addition of 50 µM ABTS in electrolyte, and dotted grey curve corresponds to the SAM. Scan rate v = 5 $mV.s^{-1}$

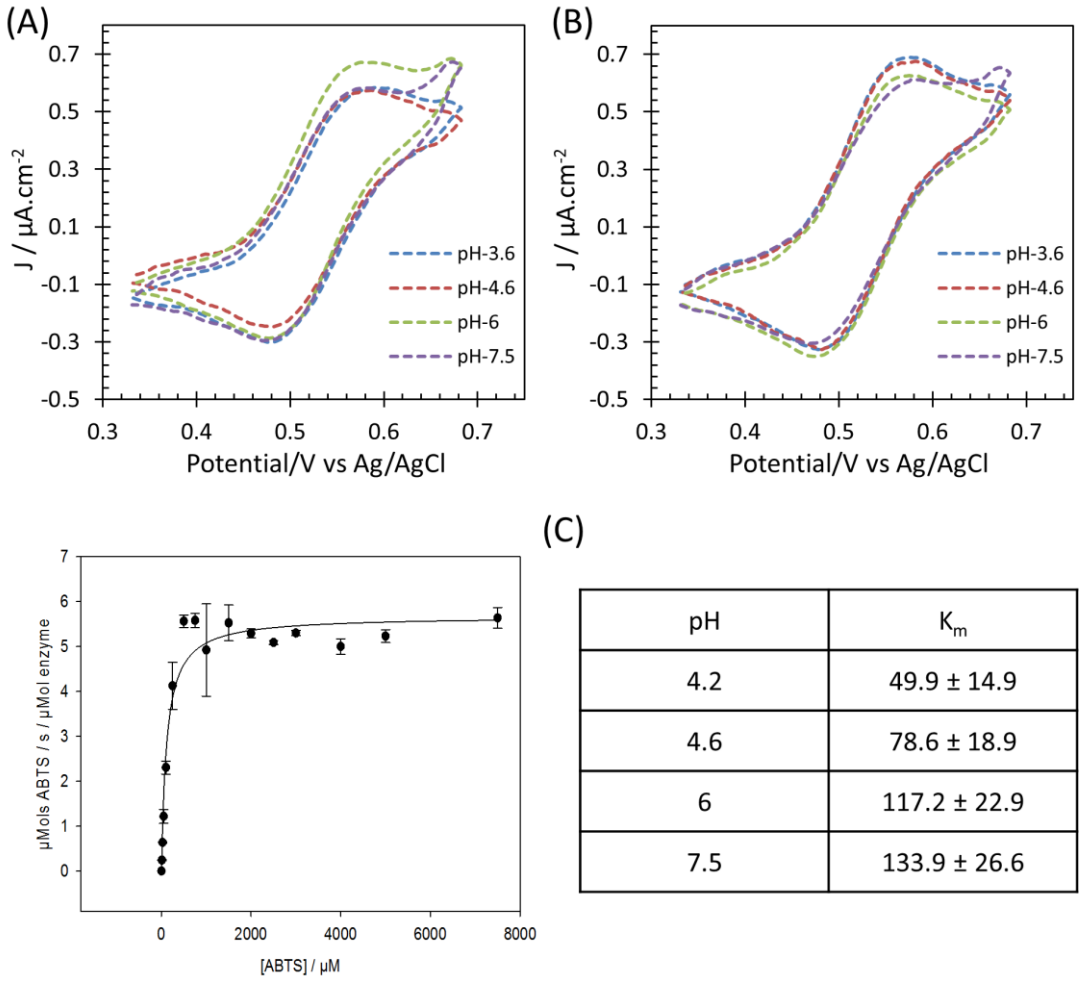

pH	K_m
4.2	49.9 ± 14.9
4.6	78.6 ± 18.9
6	117.2 ± 22.9
7.5	133.9 ± 26.6

Figure S8. Electrochemical behavior of ABTS and Michaelis-Menten (K_m) constant determination. CVs of 50 µM ABTS as a function of pH on (A) 6-MHA-SAM and (B) 4-ATP-SAM under N_2 atm. CV are recorded at 25°C and v = 5 $mV.s^{-1}$. (C) K_m determination for 300 nM *Mv* BOD as a function of pH (graph provided for pH 6) in the presence of ABTS.

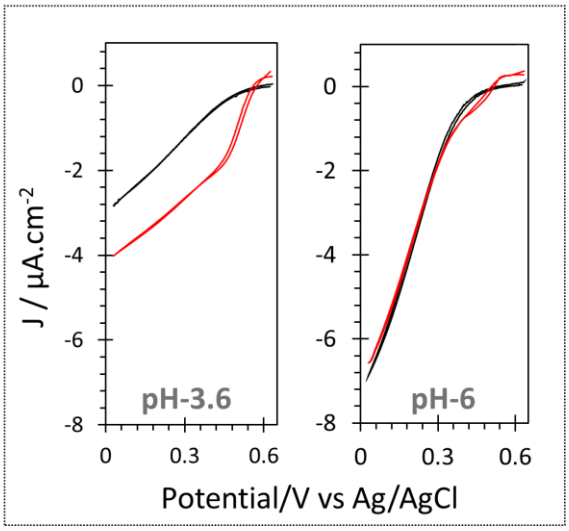

Figure S9. Electrocatalysis on 11-MUA. Catalytic O_2 reduction in different pH buffers by *Mv* BOD adsorbed at pH 6 for 15 min at 4°C on 11-MUA-SAM. Black curves and red curves are obtained before and after 50 µM ABTS in solution, respectively. v = 5 $mV.s^{-1}$.

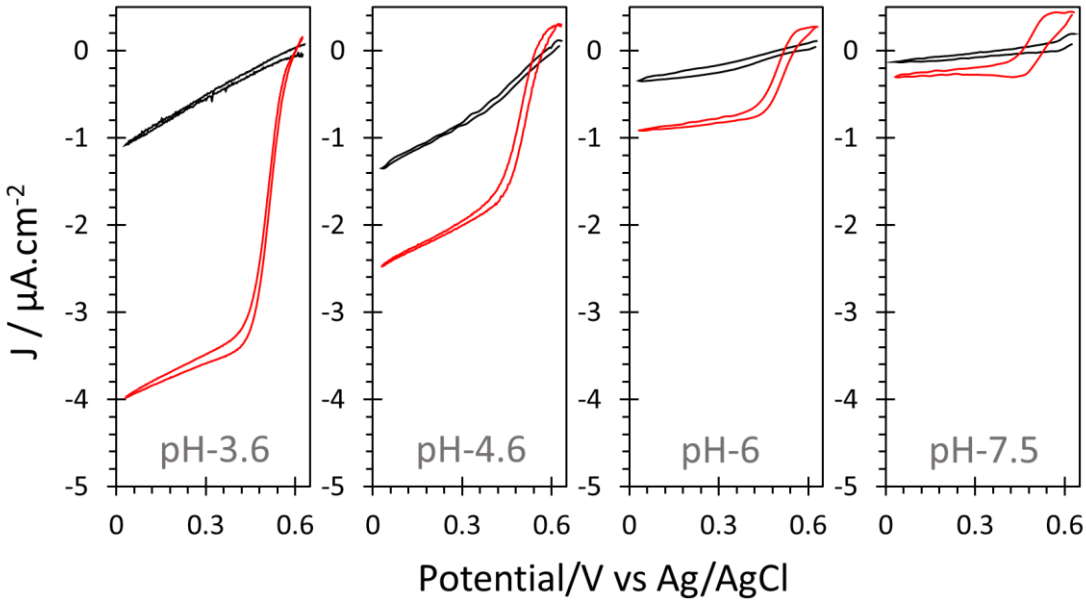

Figure S10. Electrocatalysis on butanethiol (BT). Catalytic O_2 reduction in different pH buffers by *Mv* BOD adsorbed at pH 6 for 15 min at 4°C on BT-SAM. Black curves and red curves are obtained before and after 50 µM ABTS in solution, respectively. v = 5 $mV.s^{-1}$.

Hydrophobic surfaces were also studied to validate the orientation model. On the hydrophobic BT-SAM, *Mv* BOD is able to be adsorbed, leading to coverage of 11.2±0.4, 6.5±0.4, and 5.7±0.3 at pH 3.6, 4.6, and 6, respectively (See Table S1). The surrounding of the CuT1 in *Mv* BOD was shown to be more hydrophilic than hydrophobic [2]. As a consequence, adsorption of *Mv* BOD on the hydrophobic BT-SAM at pH 6 mainly yielded a MET signal to be observed with values of 4, 2.5 and 0.9 $\mu A.cm^{-2}$ at pH 3.6, 4.6 and 6 respectively. At pH 7.5, the redox signal of ABTS alone mainly contributes to the electrochemical signal as a result of the very low activity of the enzyme.

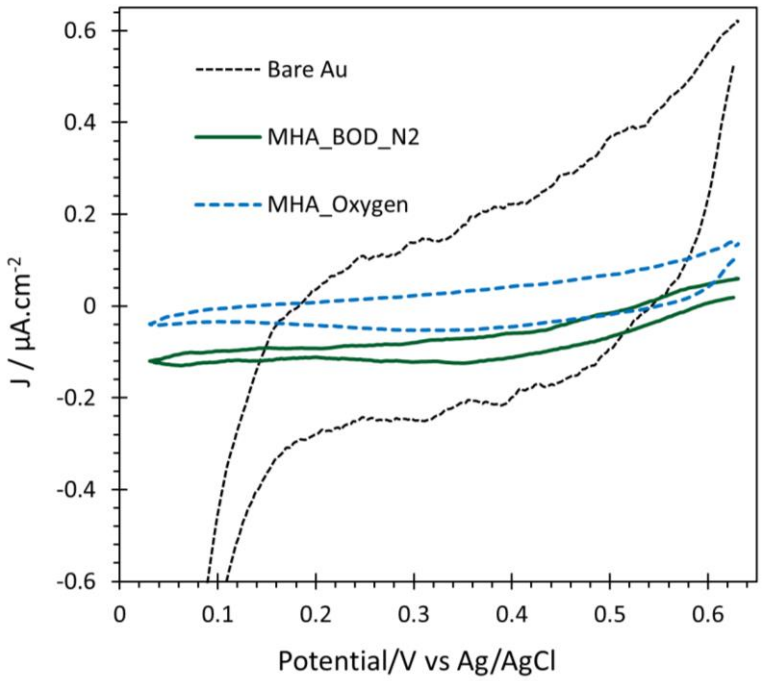

Figure S11. Control experiments on 6-MHA-SAMs. CV for 6-MHA-SAM modified (blue dotted) gold electrode under O_2 atm. CVs for unmodified (black dotted), and for 6-MHA-SAM/*Mv* BOD modified (green solid) gold electrode under N_2 atm. BOD adsorption is made at 4°C for 15 min at pH 6 and electrochemistry is made at 25°C in pH 6 buffer. Scan rate v = 5 $mV.s^{-1}$.

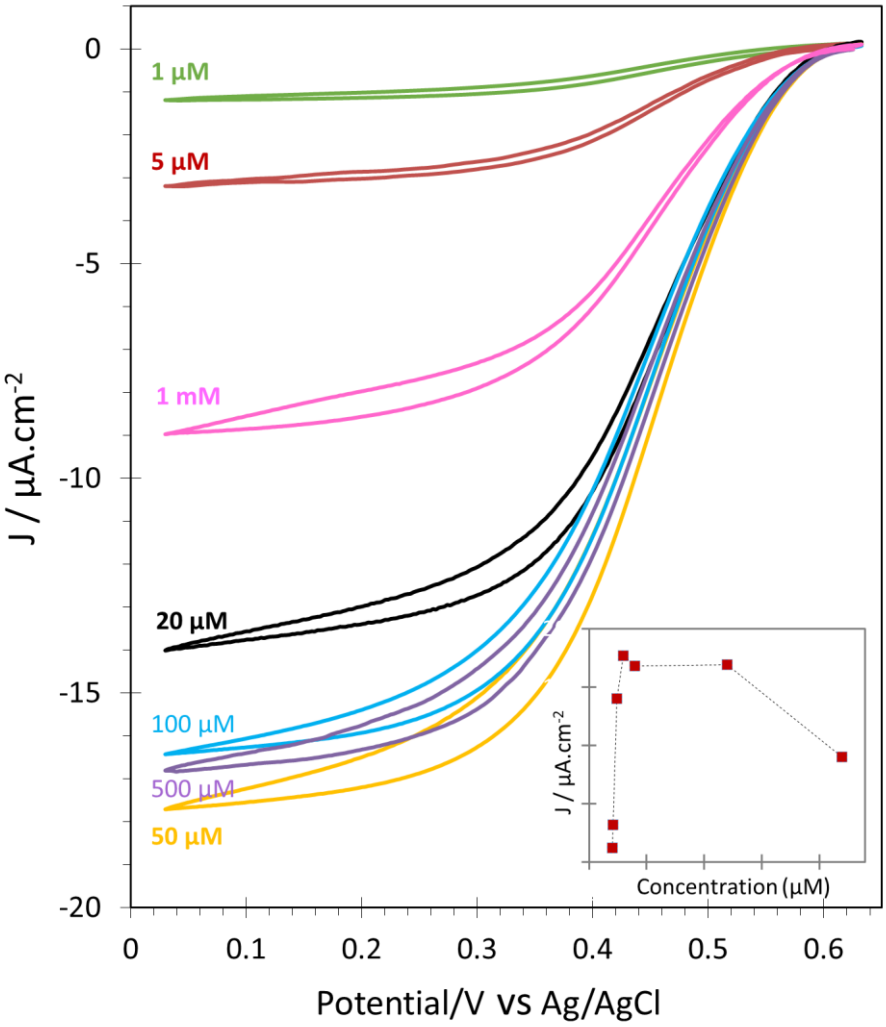

Figure S12: **Effect of *Mv* BOD concentration on the electrocatalytic activity at pH 6.**

Mv BOD concentration used for the initial adsorption step on 6-MHA-SAM is one of the parameters expected to influence the catalysis. As shown in Figure S12, the direct catalytic current for O_2 reduction first increased with the enzyme concentration to reach a plateau at a concentration around 50 µM. At concentrations higher than 600 µM, the current tends to more drastically decrease.

The amount of *Mv* BOD adsorbed on 6-MHA-SAM was quantified by SPR using the same range of *Mv* BOD concentrations as for electrocatalysis. The corresponding enzyme coverage is given in the following table (Table S2).

Table S1. SPR data for different pH of adsorption of *Mv* BOD on BT, and values of the ratio DET/DET+MET at different pHs. Catalytic currents are measured at 120 mV.

pH of ads.	BT			
	Γ_{SPR} / pmol.cm^{-2}	$I_{DET}/I_{DET+MET}$		
		pH 3.6	pH 4.6	pH 6
3.6	11.2 ± 0.4	-	-	-
4.6	6.5 ± 0.4	-	-	-
6	5.7 ± 0.3	0.24	0.48	0.34

Table S2. Relationship between enzyme coverage on 6-MHA-SAM and electroactivity for O_2 reduction. Enzyme coverage is obtained from SPR measurements at pH 6 and RT. Catalytic currents are measured at 0 V vs Ag/AgCl from Figure S12.

Mv BOD concentration / µM	Γ_{SPR} / pmol.cm^{-2}	Current density, J at 0 V vs Ag/AgCl / µA. cm^{-2}	I / Γ_{SPR} / µA.pmol^{-1}
1	3.4 ± 0.5	1.2	0.35
5	5.3 ± 0.8	3.2	0.60
20	6.3 ± 0.9	14	2.22
50	8.2 ± 1.1	17.7	2.16
100	7.7 ± 1.1	16.8	2.18
500	8.2 ± 1.2	16.9	2.05
1000	9.5 ± 1.3	9.0	0.95

The amount of total protein adsorbed shows the same tendency as the catalytic current with increasing *Mv* BOD concentrations, reaching a plateau around 50 µM. Considering that a theoretical monolayer of *Mv* BOD should be between 4.6 and 10.4 pmol.cm^{-2} depending on the conformation the enzyme takes upon immobilization (*Mv* BOD dimensions are 4x5x6 nm^3) [3], SPR data show that less than one monolayer is obtained for the lowest concentration (3.4 pmol.cm^{-2} for 1 µM). For the other concentrations, either more than one layer is formed, or a different conformation is taken by the BOD upon immobilization.

Ellipsometry conducted on 20 µM *Mv* BOD adsorbed at pH 6 gave a thickness value of 4.0±0.2 nm. Taking into account the thickness of the 6-MHA-SAM (0.7±0.05 nm)

also measured by ellipsometry, this means that the enzyme layer thickness takes a value of 3.3±0.2 nm. This suggests that the enzyme maintains its conformation at pH 6 at the SAM electrode, contrary to what was previously observed on bare gold where a low thickness value of 1.7 nm was obtained by ellipsometry [3]. The value of the catalytic current was reported to the enzyme coverage (Table S2), allowing to discuss the effect of enzyme concentration on the catalytic activity. This so-called specific activity increases up to 50 µM and remains constant till 500 µM, before decreasing for the higher enzyme concentrations. This tendency is in agreement with the QCM data reported by Blanford *et al.* which suggested that enzyme in low concentrations has time to relax and forms a more rigid adlayer displaying less activity [4]. At high enzyme concentrations, steric hindrance between immobilized proteins might be one explanation for the decrease in specific electrocatalytic activity.

Table S3. Electroactivity loss with time as a function of applied potential at different pH. % loss of the electrochemical activity recorded by chronoamperometry at different pHs under variable fixed applied potential. *Mv* BOD was adsorbed at 4°C from pH 6 buffer for 15 min and transferred to different pHs for chronoamperometry measurement at 25°C in O_2-saturated 100 mM phosphate/phosphate-citrate buffer.

pH	Activity loss % after 2700 s	
	E_{appl} = +0.13 V vs Ag/AgCl	E_{appl} = +0.53 V vs Ag/AgCl
6.5	10	20
6	2	20
5.5	5	25
4.6	0	6

References

1. Smalley, J. F.; Feldberg, S. W.; Chidsey, C. E.; Linford, M. R.; Newton, M. D.; Liu, Y.-P., The kinetics of electron transfer through ferrocene-terminated alkanethiol monolayers on gold. *J. Phys. Chem.* **1995,** *99*, 13141-13149.
2. Climent, V.; Zhang, J.; Friis, E. P.; Ostergaard, L. H.; Ulstrup, J., Voltammetry and single-molecule in situ scanning tunneling microscopy of laccases and bilirubin oxidase in electrocatalytic dioxygen reduction on Au (111) single-crystal electrodes. *J. Phys. Chem. C* **2011,** *116*, 1232-1243.
3. Pankratov, D.; Sotres, J.; Barrantes, A.; Arnebrant, T.; Shleev, S., Interfacial behavior and activity of laccase and bilirubin oxidase on bare gold surfaces. *Langmuir* **2014,** *30*, 2943-2951.
4. McArdle, T.; McNamara, T. P.; Fei, F.; Singh, K.; Blanford, C. F., Optimizing the Mass-Specific Activity of Bilirubin Oxidase Adlayers through Combined Electrochemical Quartz Crystal Microbalance and Dual Polarization Interferometry Analyses. *ACS Appl. Mater. Interfaces* **2015,** *7*, 25270-25280.